Applied Physics Research; Vol. 15, No. 1; 2023
ISSN 1916-9639 E-ISSN 1916-9647
Published by Canadian Center of Science and Education

Koudougou Station TEC's Variability Seasonal Anomalies Analysis During Fluctuating Events Over Solar Cycle 24

Tinlé Pahima[1], Doua Allain Gnabahou[1], Sibri Alphonse Sandwidi[1] & Frédéric Ouattara[1]

[1] Research Laboratory for Energy and Space Weather, University Norbert ZONGO, BP 376 Koudougou, Burkina Faso

Correspondence: Doua Allain Gnabahou, Norbert ZONGO University (UNZ), Koudougou, Burkina Faso. Tel: 226-7600-3164. E-mail: gnabahou@yahoo.fr

Received: January 25, 2023 Accepted: February 25, 2023 Online Published: March 26, 2023

doi:10.5539/apr.v15n1p50 URL: https://doi.org/10.5539/apr.v15n1p50

Abstract

This paper deals with the analysis of anomalies on variations of total electron content (TEC) during fluctuating geomagnetic events through solar cycle 24 at Koudougou station (lat 12°15'N; long:-2°20'E). Study of anomalies was done by comparing the variations of TEC during solstice and equinox seasons and variations of TEC at equinoxes to those at solstices. Comparison was made taking into account solar cycle phases and seasons influences. Equinoctial asymmetry is recorded at ascending and maximum phases. Winter anomaly is observed all night (0000 LT-04 00 LT and 2000 LT-2300 LT) at solar maximum and at all times during the ascending phase, except around 0600 LT and 1800 LT. Semi-annual asymmetry is observed during all phases of solar cycle 24 during fluctuating events.

Keywords: total electronic content, fluctuating events, solar cycle phases, seasonal anomaly

1. Introduction

Ionosphere is the ionized region of Earth's upper atmosphere located between about 50 km and 600 km. The density of plasma in ionosphere presents important variations in time (sunspot cycle, seasons, diurnal) and space (altitude, latitude, longitude) which results in a modification of ionospheric parameters such as total electron content (TEC). TEC is the number of free electrons in the ionized plasma contained in imaginary tube of $1\,m^2$ cross-section, the ends of which are bounded by orbiting satellite and ground receiver (Kersley et al. 2004). Density of F-region contributes mostly to maximum TEC that affects mainly radio waves. In the low latitude equatorial ionosphere in the F-region, ionization density distribution is characterized by a trough at equator and double peaks on either side of equator, almost at about ±15 °magnetic latitude are called the Equatorial Ionosphere Anomaly (EIA) peaks. TEC in the upper atmosphere plays a crucial role in determining range delays by electromagnetic signals as they cross the ionosphere (Rao et al. 2013). Therefore, it is important to study the TEC, as well as possible anomalies that may appear during the variations of this parameter (TEC). Observations have shown that in the low latitude region of ionosphere' F layer, electron density is subject to several anomalies among which we have: (1) winter anomaly, (2) annual anomaly, (3) semi-annual anomaly and (4) equinoctial asymmetry.

Winter anomaly is a phenomenon characterized by higher values of electron density in winter than in summer during the day; it is an anomaly that usually disappears at night (Rishbeth et al. 2000). Several mechanisms have been suggested explain it. For some authors, it could be due to changes in the composition of neutral atmosphere of the F region (Rishbeth et Edwards 1989; M. R. Torr et Torr 1973; M. Torr, Torr, et Hinteregger 1980). According to Johnson (1964) these changes could occasion an increase in the O/N_2 ratio due to convection of oxygen atoms from summer hemisphere to winter hemisphere. For others such as, Roble et al (1977) and Roble (1983) this anomalous variation in the neutral composition of F region could also be associated with seasonal variations in thermospheric winds.

Annual anomaly or non-seasonal anomaly is characterized by a preponderance of electron density of ionosphere in December compared to June. According to Buonsanto (1986) this anomaly is related to variations of intensity of solar activity according to distance Earth-Sun (the Earth being at perigee of its orbit at December solstice and at the apogee at the June solstice).

Semi-annual anomaly is a phenomenon during which electron density is higher at equinoxes than at solstices. Titheridge (1973) and Rishbeth et al (2000b) showed that the change in ratio of atomic oxygen to molecular nitrogen concentrations (O/N_2) causes the semi-annual anomaly. According to Ma et al. (2003) equatorial electrojet currents fluctuations, due to semiannual variations of diurnal tide in lower thermosphere, are the cause of variation in amplitude of equatorial ionospheric anomaly by fountain effect; which is the origin of semi-annual NmF2 anomaly in the low latitudes. Some authors attribute semi-annual variations in density of neutral components and F2 layer electrons ($NmF2$) to solar winds influence (Lal 1992; 1998). Ionospheric equinoctial asymmetry is difference in ionization between the two equinoxes (Balan et al. 1998; Bailey, Su, and Oyama 2000; Chen et al. 2012; Kawamura et al. 2002; Ouattara et al. 2017; Ren et al. 2011), despite the fact that the zenith solar angle has almost the same characteristics during these two periods (Spring and autumn).

Several authors' works on morphological characteristics of the TEC such as diurnal, monthly, seasonal, latitudinal and solar activity variation, has improved the understanding of this parameter. We have among others Walker et al (1994) Sahai et al (2007) Natali et al (2011) Akala et al (2013), De Abreu et al (2014), Zhao et al (2007), Liu et al (2013), Huo et al. (2009) and Perevalova et al. (2010), Zakharenkova et al (2013); Venkatesh et al. (2014; 2014; 2015). In addition, TEC variations have been studied in the equatorial region of Africa; for example, Ouattara et al. (2017) and Zoundi et al. (2012) have analyzed respectively equinoctial asymmetry observed in Niamey Station (Lat: 13°30' 49.18" N, Long: 2°06' 35.28" E) Center for Orbit Determination in Europe Total Electron Content (CODG TEC) variation during ~ solar cycle 23 and Koudougou station (Lat: 14.8°N; Long: 342.6°E) TEC variations during solar cycle 24 minimum phase (2009). Ouattara et al. (2017) show that Niamey CODG TEC variation follows solar cycle and present semi-annual variation with equinoctial asymmetry. And Zoundi et al. (2012) show that perturbed solar events produce positive storms and only the shock event causes a peak in the TEC at noon.

The novelty of this study is that it's the first-time seasonal anomalies in TEC variations have been analyzing at Koudougou station during fluctuating activity. The present paper aims to investigate seasonal anomalies observed during fluctuating events at Koudougou station, an African Equatorial Ionization Anomaly (EIA) region station, by using TEC values computed in this GPS station. Period of investigation covers solar cycles 24, from 2008 to 2018, and concerns the four solar phases (minimum, increasing, maximum and decreasing phases).

Section 2 is devoted to materials and methods. Section 3 presents Results and discussions and section 4 is deserved to conclusion.

2. Materials and Methods

2.1 Data

TEC data used are from Koudougou GPS station. The receiver was provided by the Ecole Nationale de Télécommunication of Bretagne (ENST Bretagne) as part of the International Heliophysical Year (IHY) project initiated by Europe-Africa Study and Research Group (GIRGEA). This receiver has been installed at University Norbert ZONGO since November 2008. TEC data recorded cover solar cycle 24, except for the years 2008; 2018 and 2019. The geomagnetic index data aa and the dates of Sudden Storm Commencement (SSC) were used (P Mayaud 1973) to elaborate the pixel diagram. This diagram represents geomagnetic index aa evolution as a function of solar activity for each Bartels rotation (Ouattara et al. 2009). The mean sunspot number (Rz) annual was used for the division of the solar cycle 24 into phases.

The geomagnetic index aa is deduced from K-index measured at two mid-latitude antipodal stations. This index measures the amplitude of global geomagnetic activity during 3-hour intervals normalized to geomagnetic latitude $\pm 50°$. It was introduced by Mayaud (1971) to monitor geomagnetic activity over the longest possible period. The daily average of the 8 tri-hourly values per day is noted Aa. An SSC corresponds to an abrupt change in the geomagnetic field followed by a geomagnetic storm that lasts less than an hour. The dates of SSCs and the values of the aa index since 1869 are available on the ISGI website (http://isgi.unistra.fr). Rz values are available on the OMNIWEB website: https://omniweb.gsfc.nasa.gov/form/dx1.html.

2.2 Geomagnetic Activities' Classification Methods

Legrand and Simon (1989); and Richardson et al. (2002; 2000) elaborated geomagnetic activities' first classification from pixel diagram. They classified geomagnetic activities into four classes: (1) quiet activities associated with slow solar winds (V < 450 km/s); (2) recurrent activities caused by fast solar winds from coronal holes (V > 450 km/s); (3) shock activities related to shock waves due to Coronal Mass Ejections (CMEs); and (4) fluctuating activities caused by fluctuations in the Sun's neutral blade. Ouattara and Amory-Mazaudier (2009) continued, in the same dynamics, by improving this method.

This classification was further improved by Zerbo et al. (2012), who pushed the limits of old classification (AC) by providing clarification of solar origin of about 20% of the geomagnetic storms in addition to the 60% explained by AC. In new classification (NC), days of quiet activity, associated with slow solar winds, correspond to days when $Aa < 20\,nT$ and disturbed activity to days when $Aa \geq 20\,nT$. Disturbed days include: i) fluctuating activity days (AFs) or fluctuating events (EFs) caused by fluctuations in the Sun's neutral blade, ii) shock events (SEs) including shock activity (SA) and cloud shock activity (CSA), and iii) recurrent event days (REs) including classical recurrent activities of AC (RAs) and Corotating Moderate Activities (CMA) due to stable corotating neutral winds.

Geomagnetic activity days selection is done using the pixel diagram (Figure 1) proposed by Simon and Legrand (1989) and improved by Ouattara and Amory-Mazaudier (2009) who organized it in columns and rows; then they defined a color code to identify different types of geomagnetic activities. A line in the diagram corresponds to a solar rotation (27 days). The SSC dates are indicated by circles surrounding the corresponding aa index value. The dates of the beginning days of Bartels cycle, the legend and the year are shown on the left, right and above the pixel diagram respectively. According to pixel diagram color code, different geomagnetic activities days are selected as follows:

1) Quiet activities (QA) corresponding to days with $Aa < 20nT$ which are represented by white and blue boxes;

2) Recurring events (RE) including:

   i) classical recurrent activities (RA) of AC corresponding to days with $Aa \geq 40nT$ and spanning one or more Bartels rotations without SSC; these days are represented by orange, red, and/or dark red boxes on at least two successive days without SSC and on at least two solar rotations;

   ii) and CMA days corresponding to days with $20nT \leq Aa < 40nT$ and spanning one or more Bartels rotations without SSC; these days are represented by yellow or green boxes on at least two successive days without SSC and on at least two solar rotations

3) Shock events (SE) including:

   i) Classical shock activities of AC (SA) corresponding to SSC days with $Aa \geq 40nT$; these days are represented by a set of 1, 2, or 3 days represented by orange, red, and/or olive-red boxes with SSC in phase beginning and no recurrence of SSC during 1, 2, 3, or 4 Bartels rotations;

   ii) and CSA days corresponding to SSC days where $20nT \leq Aa < 40nT$; these days are represented by a set of 1, 2, or 3 days represented by yellow and green boxes with SSC at phase beginning and no recurrence of SSC during 1, 2, 3, or 4 Bartels rotations

4) Fluctuating events (FE) which include all days not included in three previous classes.

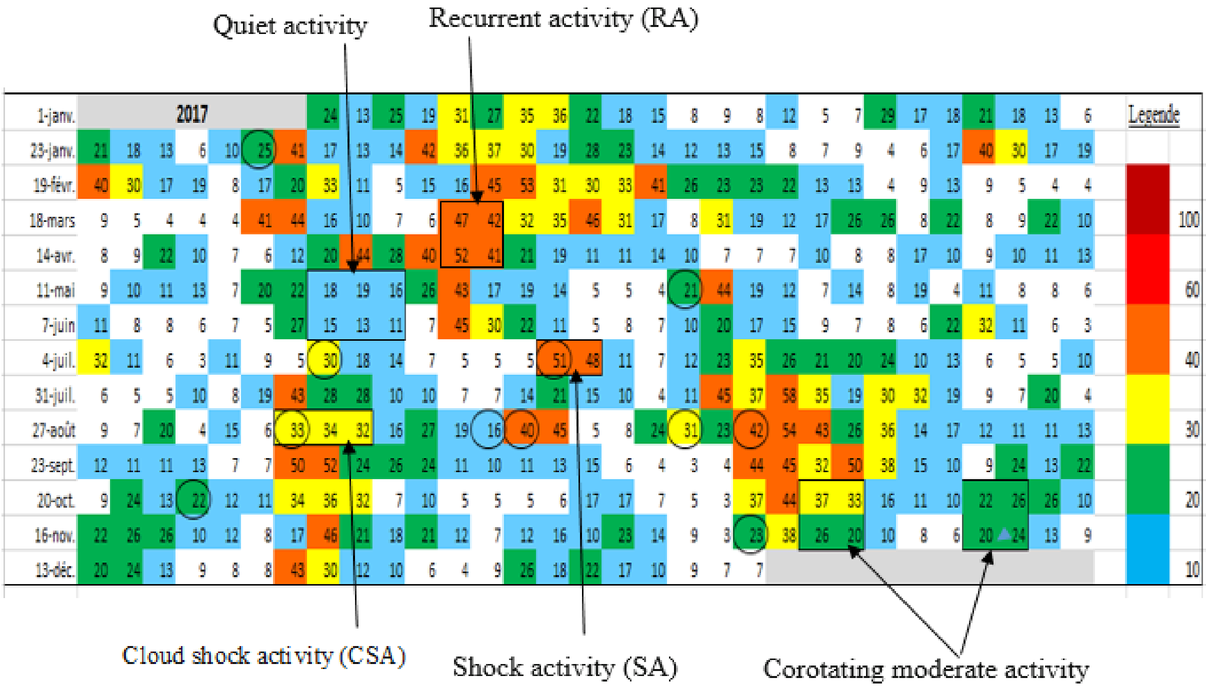

Figure 1. Pixel diagram showing the different geomagnetic activities according to the NC

2.3 Solar Phases Determination Criteria

Solar cycle is divided into phases according to criteria proposed by Ouattara and Amory-Mazaudier (2009). These criteria related to the annual average of sunspots number Rz are defined as follows: i) minimum phase: $Rz < 20$; ii) ascending phase: $20 \leq Rz \leq 100$ with Rz greater than that of previous year; iii) maximum phase: $Rz > 100$ noting that for weak solar cycles (with $Rz\,max < 100$) the years of maximum phase correspond to those with an index $Rz > 0{,}8.Rzmax$, and iv) decreasing phase: $100 \geq Rz \geq 20$ with Rz lower than that of the previous year.

However, since 2015, a new set of Rz values different from the one used by Ouattara and Amory Mazaudier (2012) is available on the OMNIWEB website (https://omniweb.gsfc.nasa.gov/form/dx1.html). Considering the previous Rz values that are limited to 2014, cycle 24 is low because its peak that corresponds to the year 2014 is less than 100 ($Rz = 78{,}9$). Since the previous Rz values ($R_{Z\_previous}$) do not exist beyond the year 2014, equations 1 and 2 were used to find the approximate values of $R_{Z\_previous}$ equivalent to those of the Rz new values (R_{Z_new}) for the missing years of cycle 24 (2015 to 2018) in order to be able to use the criteria of Ouattara and Amory-Mazaudier (2012). Table 1 summarizes solar cycle 24' previous, new and approximate Rz values.

$$\sigma_1 = \frac{R_{Zancien}}{R_{Znouveau}} \quad \text{(eq 1)}$$

$$\sigma_2 = \frac{\sum_{2008}^{2014} \sigma_1}{7} \quad \text{(eq 2)}$$

Equation 2 gives $\sigma_2 = 0{,}679709088$

$R_{Z\_approximate}$ is the approximate value of $R_{Z\_previous}$. It's estimated by the equation (3).

$$R_{Z\_approximate} = R_{Znew} \times \sigma_2 \,. \quad \text{(eq 3)}$$

Table 1. Previous, new and approximate annual average Rz values

Years	2008	2009	2010	2011	2012	2013	2014	2015	2016	2017	2018
$R_{Z\ old}$	2.9	3.1	16.5	55.7	57.7	64.9	78.9				
$R_{Z\ new}$	4.2	4.8	24.9	80.8	84.5	94	113.3	69.8	39.8	7	3.6
$R_{Z\ app\_old}$								47.4	27.1	14.7	4.8

Table 2 shows results of solar cycle 24 cutting into phases.

Table 2. Results of solar cycle 24 cutting into phases

Phases	Corresponding years
Minimum	2008; 2009 and 2010
Ascending	2011 and 2012
Maximum	2013 et 2014
Descending	2015; 2016; 2017 and 2018

2.4 Seasons Determination Criteria

Several studies have demonstrated the seasonal dependence of TEC variability. Some have revealed the existence of semi-annual variations characterized by electron density peaks at equinoxes (Huang et Cheng 1996; Zou et al. 2000; Rishbeth et al. 2000a; Araujo-Pradere et al. 2011); while others have revealed the existence of winter anomaly characterized by peaks in winter compared to summer (Huang et Cheng 1996; Zou et al. 2000; Rishbeth et al. 2000a; Araujo-Pradere et al. 2011). There are four seasons in the year: (1) spring (March, April, and May); (2) summer (June, July, and August); (3) fall (September, October, and November); and (4) winter (December, January, and February). But for the present study, seasons of equinoxes are spring or equinox of March noted M-A (March and April) and autumn or equinox of September noted S-O (September and October) and seasons of solstices are summer or the solstice of June noted J-J (June and July) and winter or solstice of December noted D-J (December and January).

2.5 Data Analysis Methods

The error bars placed on TEC profiles of the QA, for the qualitative analysis of FE compared to QA, are obtained by $\delta = \sqrt{V}$ where V is the variance given by equation 4.

$$V = \frac{\sum_{i=1}^{N}(TEC_i - \overline{TEC})^2}{N} \qquad \text{(eq. 4)}$$

With TEC_i the hourly values of TEC; $\overline{TEC}$ the average hourly value of daily hourly values and N the total number of days depending on solar phase or season considered.

The solar cycle 24's (January 1, 2008 to December 31, 2018) FE and QA days were counted in order to analyze their occurrences. The study included 2939 QA days and 697 FE days. The occurrence rates are obtained using the formula in Equation 6.

$$\%Occ = \frac{N_A}{N_T} \times 100 \qquad \text{(eq 5)}$$

Where N_A is the number of QA or FE days per solar phase or season considered and N_T is the total number of days per solar phase or by the considered season.

Quantitative analysis using relative deviation of the TEC (δTEC) allows to appreciate the intensity of the observed anomaly. The relative deviation of TEC is defined by equation 6.

$$\delta TEC = \frac{x_i^F - x_i^L}{x_i^L} \times 100 \qquad \text{(eq 6)}$$

Where the x_i^F represent the hourly average TEC values during March equinox (M-A) or June solstice (J-J) and the x_i^L those during the September equinox (S-O) or December solstice (D-J). If δTEC is within ∓20%, the skewness is said to be insignificant; otherwise, the conclusion is that a clear skewness exists.

3. Results and Discussions

3.1 Results

3.1.1 Occurrence of Fluctuating Activities by Season and Solar Phase

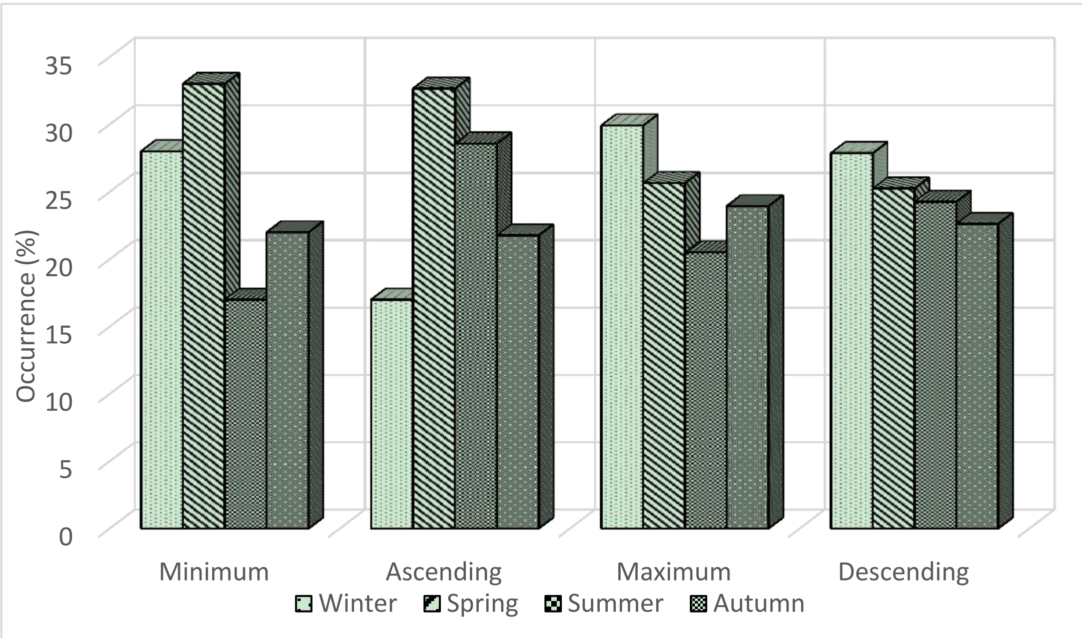

Figure 2. Variability in occurrence of fluctuating events by solar phase and season

Figure 3 shows the occurrence of FEs by season and by solar phase. At solar minimum FEs occurrence decreased from spring (33%) to summer (17%) and increase in autumn (22%) and in winter (28%). In the descending phase FEs are predominant in spring season (32.65%) followed by summer season (28.57%). A low occurrence of FEs is recorded in autumn (21.77%) and winter (17%). During the maximum phase more FEs days are recorded in winter (29.91%). In spring and autumn, the number of FEs days is low with an occurrence rate of 25.64% and 23.93% respectively. Lowest occurrence of FEs is recorded in summer. During the decreasing phase, FEs days appear in a decreasing manner in winter (27.87%), spring (25.25%), summer (24.26%), and fall (22.62%). In general, EF days appear more in spring during the minimum and ascending phases; in winter during the maximum and descending phases.

3.1.2 Seasonal Anomalies Analysis on TEC Variations per Solar Phase

Figure 3 through Figure 6 show diurnal seasonal variations in TEC and relative deviation δTEC profiles between seasons during minimum, ascending, maximum and descending solar phases. These plots are related to study equinoctial (panel "a"), winter (panel "b") and semi-annual (panel "c") anomalies on TEC variations at Koudougou station during solar cycle 24. At solar minimum (Figure 3), the study is devoted only to semi-annual anomaly analysis because during this phase there is a lack of TEC data for FEs days of summer and autumn seasons.

3.1.2.1 Seasonal Anomalies Analysis on TEC Variations at Solar Minimum

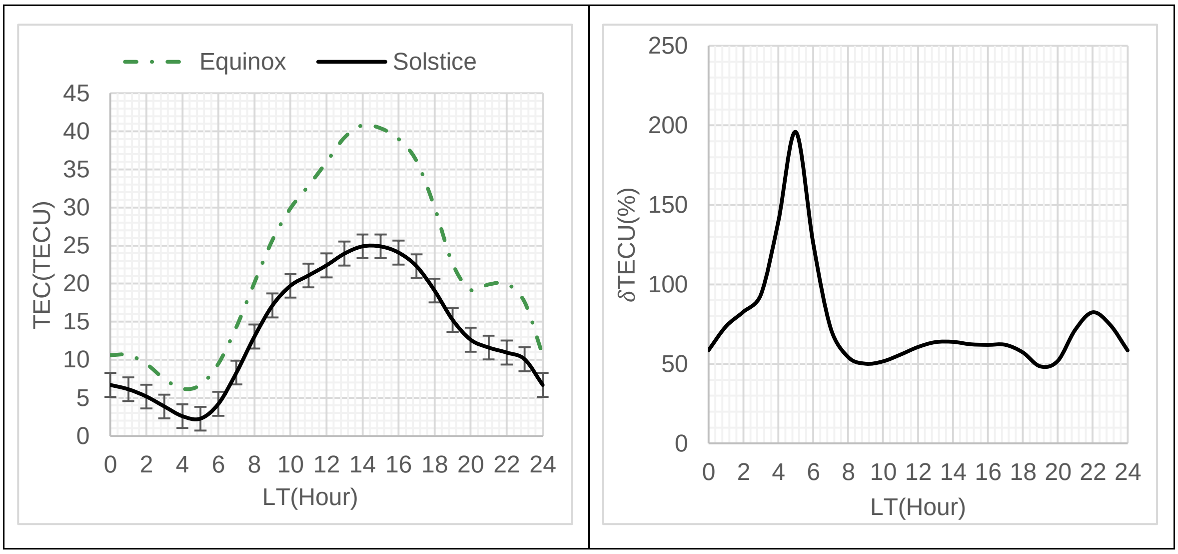

Figure 3. TEC diurnal seasonal variations profiles at solar minimum

Figure 3 shows TEC variations during FEs at equinoxes and solstices. Error bars show that ionization is different at the two seasons almost all the time. Equinox curve is above the solstice curve all the time, testifying the presence of semi-annual asymmetry. δTEC curve shows values above +20% at all times. At minimum phase, there is semi-annual asymmetry on the PRE phenomenon and on diurnal TEC variations profiles but this asymmetry is absent on the $E \times B$ drift.

3.1.2.2 Seasonal Anomalies Analysis on TEC Variations at Ascending Phase

a

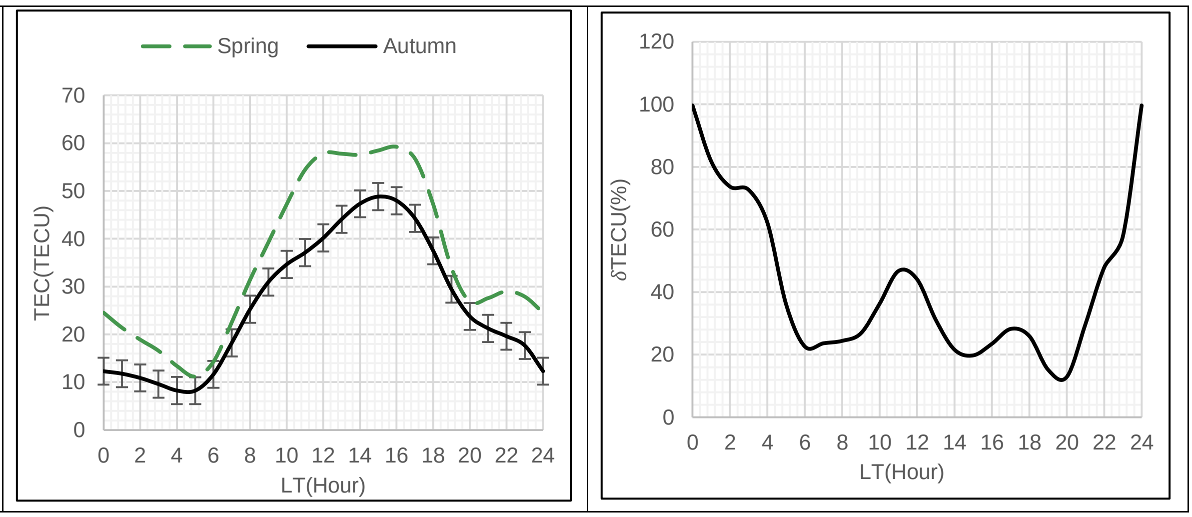

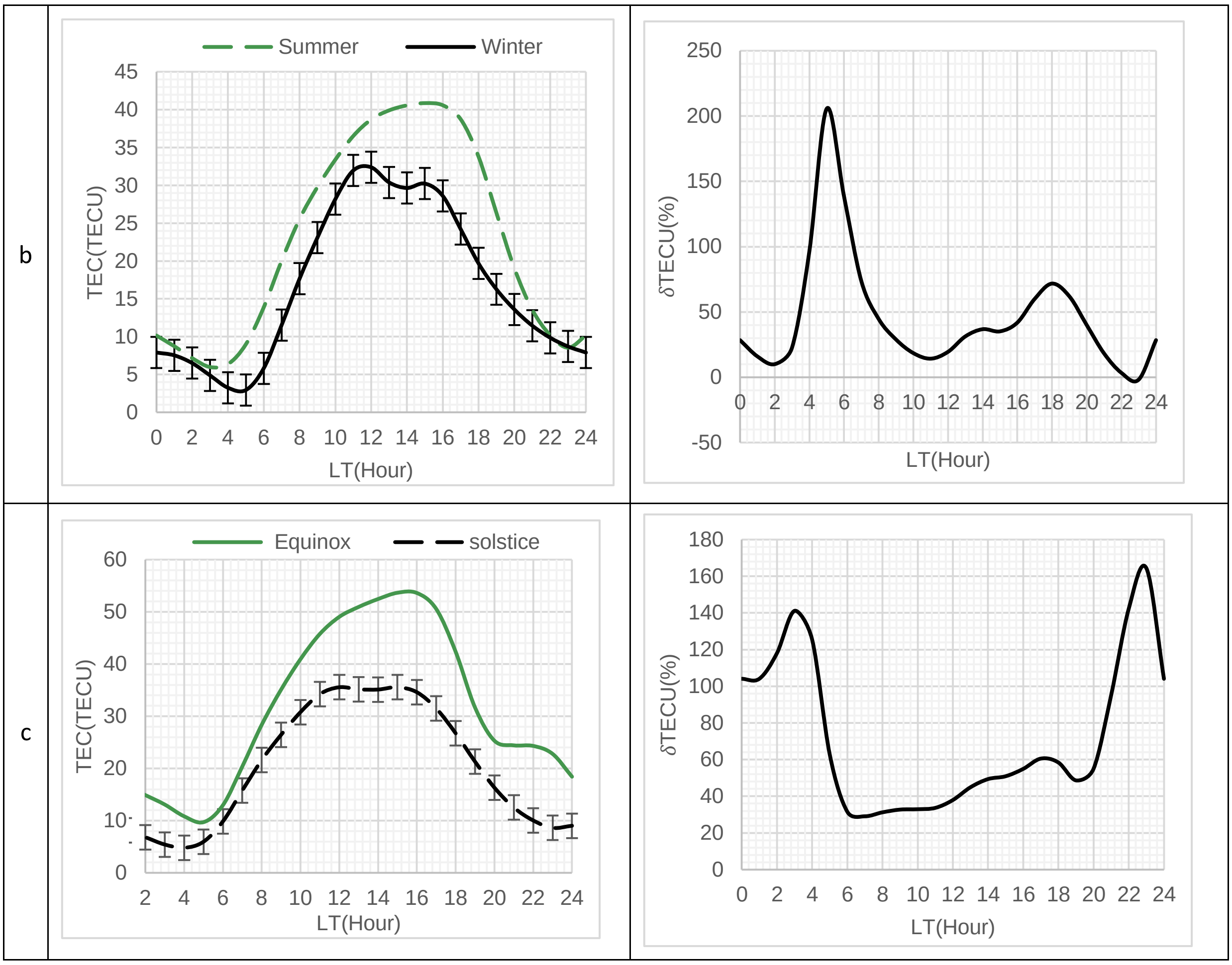

Figure 4. TEC seasonal diurnal variations profiles at ascending phase

In Figure 4"a", We note that at the equinoxes, the TEC plot shows a trough around noon and a night peak (2200 LT) in the spring, reflecting the presence of equinoctial asymmetry on the $E \times B$ drift and on the PRE. Furthermore, the error bars show that the ionization is, at all times, different at the two equinoxes testifying to the presence of equinoctial asymmetry. δTEC curve shows values greater than 20% all the time except at 1500 LT and 2000LT; the maximum difference between the two equinoxes is located at 0000 LT with a peak $\delta TEC = 99.63\%$. This shows a clear presence of equinoctial asymmetry at the rising phase throughout the day. However, the asymmetry is less important around 1500 and 2000 LT.

In Figure 4"b", The TEC graphs show the presence of annual asymmetry on $E \times B$ upward drift of plasma which results in the presence of a trough around noon only in summer. Absence of annual asymmetry on the PRE is noted because both graphs (winter, summer) have similar evolution at night. Error bars show the absence of a winter anomaly in the TEC at all times which is reflected in larger TEC values in summer than in winter. δTEC values exceed 20% at all times except between [0100 LT - 0200LT], [1000 LT - 1200LT] and [2100 LT - 2300LT] where the δTEC values are between ∓20%. From these observations we note the almost complete absence of winter anomaly on the TEC at the ascending phase.

In Figure 4"c", the TEC graphs show, on the one hand, the absence of semi-annual asymmetry on the $E \times B$ upward drift which translates into the absence of ionization troughs at the solstices and equinoxes and, on the other hand, the existence of semi-annual asymmetry on the PRE which translates into the presence of a night peak only at the equinoxes. Error bars show that the ionization is different at both seasons at all times. Equinox curve is above the solstice curve all the time, testifying to the presence of semi-annual asymmetry. δTEC curve has values greater than +20% at all times. Then, there is the absence of semi-annual asymmetry on the $E \times B$ drift, and its existence on the evening ionization peak and on the diurnal TEC variation profiles.

3.1.2.3 Seasonal Anomalies on TEC Variations at Solar Maximum

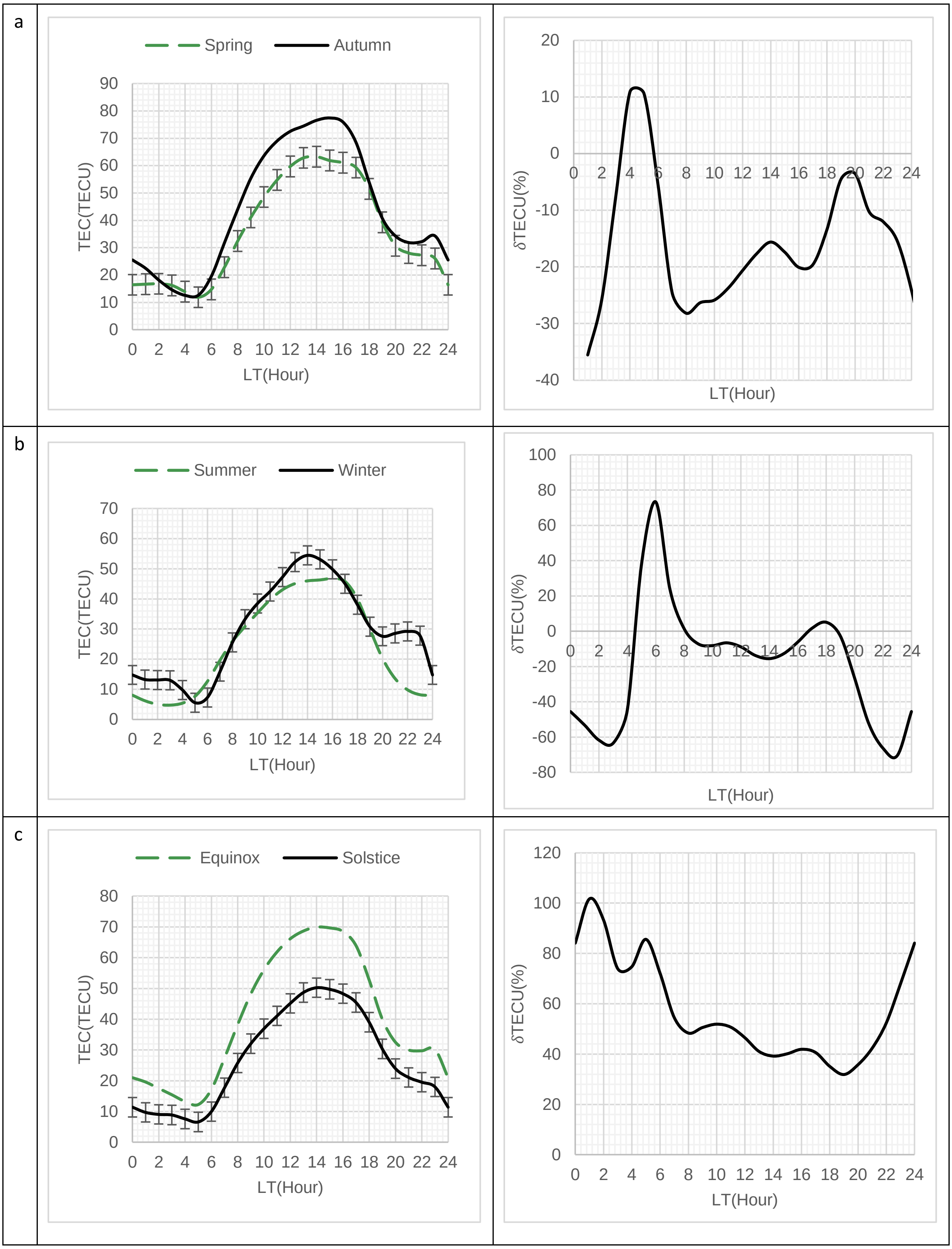

Figure 5. Profiles of diurnal seasonal variations of TEC at solar maximum

In Figure 5"a" an absence of noon troughs at equinoxes (spring, fall) and the presence of night peaks only in spring are observed; thus, reflecting the absence of equinoctial asymmetry on the $E \times B$ drift at equinoxes (spring, fall) and the presence of equinoctial asymmetry on the PRE. Error bars show that the ionization is, at all times, different at both equinoxes testifying the presence of equinoctial asymmetry. On the other hand, δTEC present values between $\pm 20\%$ before sunrise (0300 LT - 0600LT) and from 1300 LT to 2300LT. Therefore, the equinoctial asymmetry on the TEC variations is considerable at all times except at the hours mentioned above during the maximum phase.

Graphs in Figure 5 "b", show the absence of semi-annual asymmetry on the $E \times B$ drift (no ionization dip in winter and summer) and the existence of this asymmetry on the PRE (night peak only in summer ($27.81\ TECU$). Winter curve is above the summer curve all the time except in the morning (0500 LT-0800 LT) and evening (1700 LT-1800 LT). Error bars show that the ionization is different at both solstices at all times. δTEC curve shows that there is a winter anomaly with δTEC values less than -20% between 0000 LT and 0400 LT and from 2000 LT to 2300 LT. Indeed, the absence of winter anomaly is observed between 0500 LT and 0600 LT as δTEC values are greater than +20%. Thus, at solar maximum, the winter anomaly is observed on TEC variations almost all night (0000-0400 LT and from 2000-2300 LT).

Panel "c" of figure 5 shows the existence of semi-annual asymmetry on the PRE (nighttime peak observed only at equinoxes). Error bars show that the ionization is different at both seasons all the time. Equinox curve is above the solstice curve all the time, testifying to the presence of semi-annual asymmetry on the variations of TEC. Positive values of δTEC all the time confirm this observation with values above $+20\%$ all the time indicating that the phenomenon is very important at solar maximum.

3.1.2.4 Seasonal Anomalies on the Variability of TEC in the Downward Phase

Graphs in Figure 6 "a" show the absence of equinoctial asymmetry on the $E \times B$ drift as well as on the evening ionization peak. Error bars show that the ionization is different in the two seasons at all times. Spring curve is above the fall curve all the time, testifying the absence of the equinoctial asymmetry. δTEC values are positive all the time and greater than +20% around 0000 LT at 0600 LT and from 2200 to 2300 LT indicating the period when the asymmetry is intense.

a

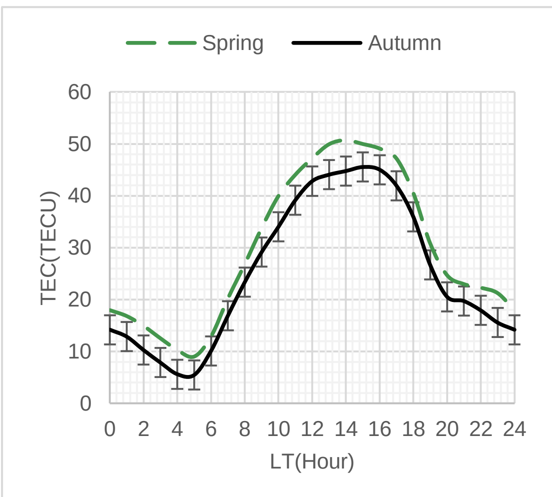

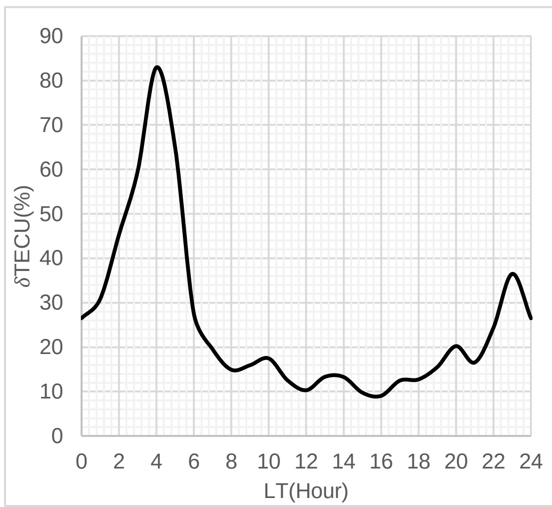

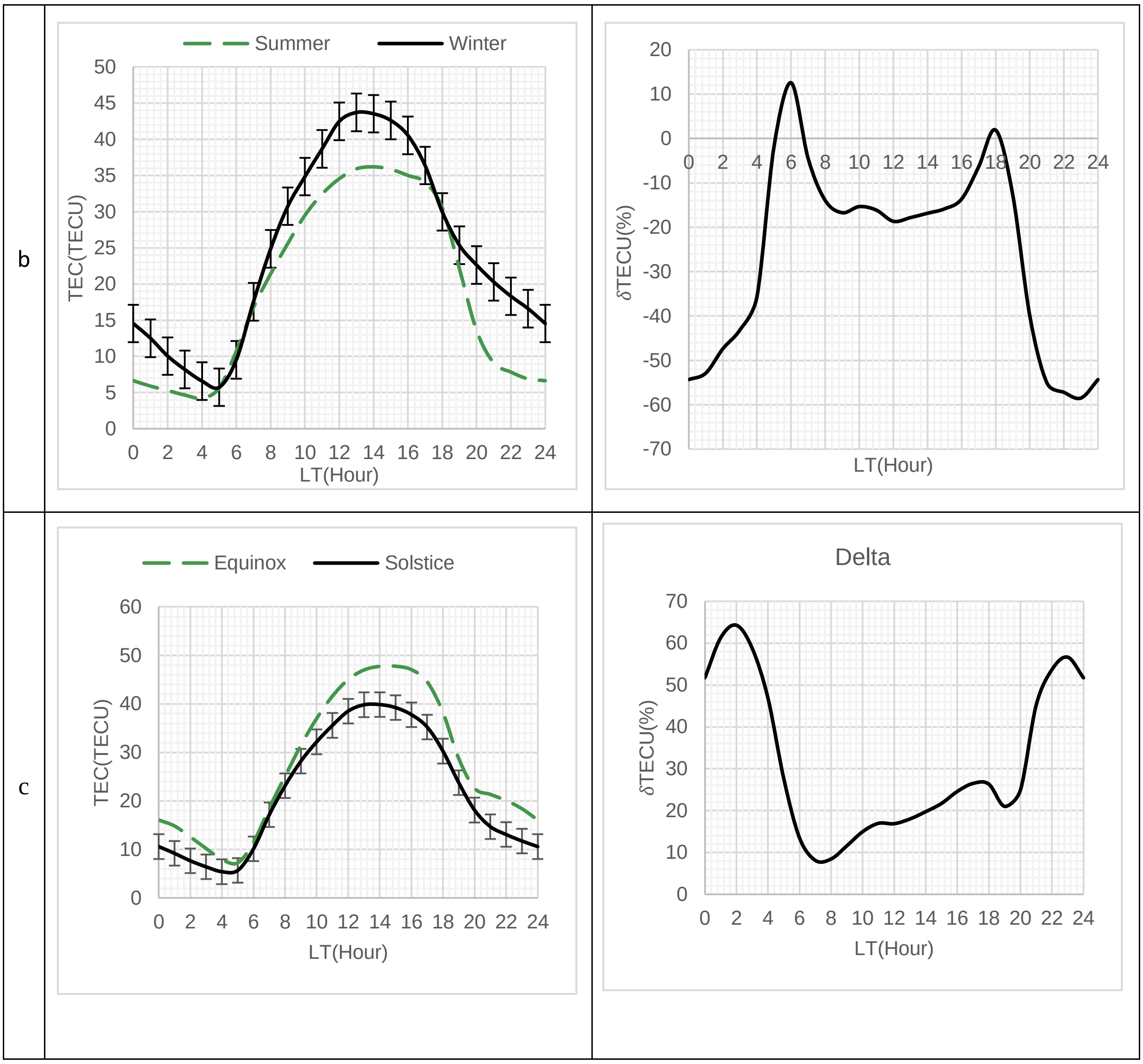

Figure 6. Profiles of diurnal seasonal variations of TEC at the descending phase

On Figure 6 "b" the graphs show the absence of winter anomaly on $E \times B$ and on the PRE. Error bars show that ionization is different in both seasons at all times. Winter curve is above the summer curve all the time except in the morning (0600 LT) and evening (1800 LT), testifying to the presence of the winter anomaly at the solstices except at 0600 LT and 1800 LT. δTEC values are lower than -20% between 0000 LT and 0400 LT and from 2000 LT to 2300 LT showing that at this period the phenomenon is intense.

Figure 6. "c", shows the absence of semi-annual asymmetry in $E \times B$ and PRE. Error bars show that the ionization is different at the two seasons at all times. Equinox curve is above the solstice curve all the time, showing the presence of the semi-annual asymmetry on the variations of the TEC. δTEC curve shows values greater than +20% from 0000 LT to 0500 LT and from 1500 LT to 2300 LT showing that at this period the asymmetry is considerable. In sum, there is the absence of semi-annual asymmetry on the $E \times B$ drift, on the evening ionization peak, and the presence of this asymmetry on the diurnal TEC variation profiles during the downward phase.

3.2 Discussion

From the analysis of possible seasonal anomalies on TEC diurnal variations during FEs, it appears that:

(1) Equinoctial asymmetry is observed at the ascending phase and solar maximum. On a seasonal scale, FEs predominate in spring than in autumn during the ascending phase and at solar maximum. This suggests that on the solar phase scale, the presence of equinoctial asymmetry is not related to

occurrence of FE days. Balan et al (1998) suggest that the asymmetric variation of the temperature and composition of thermospheric winds would be at the origin the equinoctial asymmetry of ionospheric plasma density. In addition, the work of Ouattara et al. (2017) at Niamey station (lat. 13.3 °N; long. 2.0 ° E) showed that the Russell McPherron mechanism is a cause of the equinoctial asymmetry of the TEC.

(2) At solar maximum the winter anomaly is present all night (0000 LT-0400 LT) and from (2000 LT-2300 LT); and during the descending phase it is observed all the time except at 0600 LT and 1800 LT. Contrary to the observation of Rishbeth et al., (2000b) which shows that the winter anomaly disappears at night. On a seasonal scale, FEs predominate in winter than in summer at maximum and at downward phases. This shows that on the scale of solar phases and seasons, the presence of anomaly is related on the one hand to the occurrence of FE days. On other hand, this anomaly could be due to changes in the composition of the neutral atmosphere of F-ionospheric region (Rishbeth et Edwards 1989; M. R. Torr et Torr 1973; M. Torr, Torr, et Hinteregger 1980). And according to Johnson (1964), these changes could occasion an increase in the ratio of O/N_2; due to convection of oxygen atoms from the summer to the winter hemisphere.

(3) Semi-annual asymmetry is observed during all phases of solar cycle 24 during fluctuating events. It is most pronounced at low and mid-latitudes (M. R. Torr et Torr 1973; Yonezawa 1971). Anomaly is related to the variation in the temperature of the Earth's upper atmosphere Yonezawa (1971). According to Mahajan (1971) and Torr and Torr (1973) it is due to semi-annual variation in the density of neutral atmosphere at low altitudes related to geomagnetic and auroral activities. On other hand, Rishbeth et al. (2000b) showed that the change in ratio of atomic oxygen to molecular nitrogen concentrations (O/N_2) causes the semi-annual anomaly.

4. Conclusion

Anomalies analysis on TEC diurnal variations during FEs of solar cycle 24 at station of Koudougou, showed the presence of equinoctial asymmetry at the ascending phase and at the phase maximum. The winter anomaly is observed all night (0000 LT-0400 LT) and from 2000 LT to 2300 LT at solar maximum and all the time except around 0600 LT and 1800 LT at the ascending phase. Semi-annual asymmetry is observed during all solar phases. From the analysis of Fes occurrences by season and by solar phase, it is generally found that they appear more in spring, at minimum and ascending phases. They predominate in winter during maximum and descending phases. Equinoctial asymmetry is therefore not related to FEs occurrences, which is not the case for the winter anomaly.

Data Availability

The sunspot data used to support the findings of our study are available at: https://www.sidc.be/silso/datafiles. The geomagnetic aa index data are available at https://isgi.unistra.fr/data_download.php.

Conflicts of Interest

The authors declare no conflicts of interest.

Acknowledgments

The authors thank Rolland Fleury from IMT Bretagne, Technopole, Brest Iroise, France for his cooperation by providing Koudougou TEC data.

References

Akala, A., Seemala, G., Doherty, P., Valladares, C., Carrano, C., Espinoza, J., & Oluyo, S. (2013). *Comparison of equatorial GPS-TEC observations over an African station and an American station during the minimum and ascending phases of solar cycle 24* (pp. 2085-2096). Presented at the Annales Geophysicae, Copernicus GmbH. https://doi.org/10.5194/angeo-31-2085-2013

Bailey, G., Su, Y., & Oyama, K.-I. (2000). *Yearly variations in the low-latitude topside ionosphere* (pp. 789-798). Presented at the Annales Geophysicae, Copernicus GmbH. https://doi.org/10.1007/s00585-000-0789-0

Balan, N., Batista, I., Abdu, M., MacDougall, J., & Bailey, G. (1998). Physical mechanism and statistics of occurrence of an additional layer in the equatorial ionosphere. *Journal of Geophysical Research: Space Physics*, *103*(A12), 29169-29181. https://doi.org/10.1029/98JA02823

Balan, N., Otsuka, Y., Bailey, G., & Fukao, S. (1998). Equinoctial asymmetries in the ionosphere and thermosphere observed by the MU radar. *Journal of Geophysical Research: Space Physics*, *103*(A5), 9481-9495. https://doi.org/10.1029/97JA03137

Balan, N., Souza, J., & Bailey, G. J. (2018). Recent developments in the understanding of equatorial ionization anomaly: A review. *Journal of Atmospheric and Solar-Terrestrial Physics*, *171*, 3-11. https://doi.org/10.1016/j.jastp.2017.06.020

Buonsanto, M. (1986). Seasonal variations of day-time ionisation flows inferred from a comparison of calculated and observed NmF2. *Journal of Atmospheric and Terrestrial Physics*, *48*(4), 365-373. https://doi.org/10.1016/0021-9169(86)90004-8

Chen, Y., Liu, L., & Wan, W. (2011). Does the F10. 7 index correctly describe solar EUV flux during the deep solar minimum of 2007-2009?. *Journal of Geophysical Research: Space Physics*, *116*(A4). https://doi.org/10.1029/2010JA016301

Chen, Y., Liu, L., Wan, W., & Ren, Z. (2012). *Equinoctial asymmetry in solar activity variations of NmF2 and TEC* (pp. 613-622). Presented at the Annales geophysicae, Copernicus GmbH. https://doi.org/10.5194/angeo-30-613-2012

De Abreu, A., Fagundes, P., Gende, M., Bolaji, O., De Jesus, R., & Brunini, C. (2014). Investigation of ionospheric response to two moderate geomagnetic storms using GPS–TEC measurements in the South American and African sectors during the ascending phase of solar cycle 24. *Advances in Space Research*, *53*(9), 1313-1328. https://doi.org/10.1016/j.asr.2014.02.011

Frederic, O. (2011). Variability of CODG TEC and IRI 2001 total electron content (TEC) during IHY campaign period (21 March to 16 April 2008) at Niamey under different geomagnetic activity conditions. *Scientific Research and Essays, 6*(17), 3609-3622. https://doi.org/10.5897/SRE10.1050

Hernandez, G., & Roble, R. (1977). Direct measurements of nighttime thermospheric winds and temperatures, 3. Monthly variations during solar minimum. *Journal of Geophysical Research*, *82*(35), 5505-5511. https://doi.org/10.1029/JA082i035p05505

Horning, E., Horning, M., Carroll, D., Dzidic, I., & Stillwell, R. (1973). New picogram detection system based on a mass spectrometer with an external ionization source at atmospheric pressure. *Analytical Chemistry*, *45*(6), 936-943. https://doi.org/10.1021/ac60328a035

Huo, X., Yuan, Y., Ou, J., Zhang, K., & Bailey, G. (2009). Monitoring the global-scale winter anomaly of total electron contents using GPS data. *Earth, Planets and Space*, *61*(8), 1019-1024. https://doi.org/10.1186/BF03352952

Johnson, F. S. (1973). Horizontal variations in thermospheric composition. *Reviews of Geophysics*, *11*(3), 741-754. https://doi.org/10.1029/RG011i003p00741

Kawamura, S., Balan, N., Otsuka, Y., & Fukao, S. (2002). Annual and semiannual variations of the midlatitude ionosphere under low solar activity. *Journal of Geophysical Research: Space Physics*, *107*(A8), SIA-8. https://doi.org/10.1029/2001JA000267

Lal, C. (1992). Global F2 layer ionization and geomagnetic activity. *Journal of Geophysical Research: Space Physics*, *97*(A8), 12153-12159. https://doi.org/10.1029/92JA00325

Lal, C. (1998). Solar wind and equinoctial maxima in geophysical phenomena. *Journal of Atmospheric and Solar-Terrestrial Physics*, *60*(10), 1017-1024. https://doi.org/10.1016/S1364-6826(98)00046-7

Legrand, J.-P., & Simon, P. (1985). Some solar cycle phenomena related to the geomagnetic activity from 1868 to 1980. I-The shock events, or the interplanetary expansion of the toroidal field. *Astronomy and Astrophysics*, *152*, 199-204.

Liu, G., Huang, W., Gong, J., & Shen, H. (2013). Seasonal variability of GPS-VTEC and model during low solar activity period (2006–2007) near the equatorial ionization anomaly crest location in Chinese zone. *Advances in Space Research*, *51*(3), 366-376. https://doi.org/10.1016/j.asr.2012.09.002

Ma, R., Xu, J., & Liao, H. (2003). The features and a possible mechanism of semiannual variation in the peak electron density of the low latitude F2 layer. *Journal of Atmospheric and Solar-Terrestrial Physics*, *65*(1), 47-57. https://doi.org/10.1016/S1364-6826(02)00192-X

Mayr, H., & Mahajan, K. (1971). Seasonal variation in the F 2 region. *Journal of Geophysical Research*, *76*(4), 1017-1027. https://doi.org/10.1029/JA076i004p01017

McDonald, F. B., Moraal, H., Reinecke, J., Lal, N., & McGuire, R. E. (1992). The cosmic radiation in the heliosphere at successive solar minima. *Journal of Geophysical Research: Space Physics*, *97*(A2), 1557-1570. https://doi.org/10.1029/91JA02389

Mendillo, M., Huang, C.-L., Pi, X., Rishbeth, H., & Meier, R. (2005). The global ionospheric asymmetry in total electron content. *Journal of Atmospheric and Solar-Terrestrial Physics*, *67*(15), 1377-1387. https://doi.org/10.1016/j.jastp.2005.06.021

Natali, M. P., & Meza, A. (2011). *Annual and semiannual variations of vertical total electron content during high solar activity based on GPS observations* (pp. 865-873). Presented at the Annales Geophysicae, Copernicus GmbH. https://doi.org/10.5194/angeo-29-865-2011

Opio, P., D'ujanga, F., & Ssenyonga, T. (2015). Latitudinal variation of the ionosphere in the African sector using GPS TEC data. *Advances in Space Research*, *55*(6), 1640-1650. https://doi.org/10.1016/j.asr.2014.12.036

Ouattara, F., Zerbo, J.-L., Kabor, M., & Fleury, R. (2017). Investigation on equinoctial asymmetry observed in Niamey Station Center for Orbit Determination in Europe Total Electron Content (CODG TEC) variation during~ solar cycle 23. *International Journal of Physical Sciences*, *12*(22), 308-321. https://doi.org/10.5897/IJPS2017.4684

Perevalova, N., Polyakova, A., & Zalizovski, A. (2010). Diurnal variations of the total electron content under quiet helio-geomagnetic conditions. *Journal of Atmospheric and Solar-Terrestrial Physics*, *72*(13), 997-1007. https://doi.org/10.1016/j.jastp.2010.05.014

Picanço, G. A. S., Denardini, C. M., Nogueira, P. A. B., Resende, L. C. A., Carmo, C. S., Chen, S. S., … Romero-Hernandez, E. (2022). Study of the equatorial and low-latitude TEC response to plasma bubbles during the solar cycle 24-25 over the Brazilian region using a Disturbance Ionosphere indeX. *Annales Geophysicae Discussions*, 1-29. https://doi.org/10.5194/angeo-2021-71

Rao, P. R., Venkatesh, K., Prasad, D., & Niranjan, K. (2013). On the uncertainties in the measurement of absolute (true) TEC over Indian equatorial and low latitude sectors. *Advances in Space Research*, *51*(7), 1238-1252. https://doi.org/10.1016/j.asr.2012.10.032

Rees, M., Emery, B., Roble, R., & Stamnes, K. (1983). Neutral and ion gas heating by auroral electron precipitation. *Journal of Geophysical Research: Space Physics*, *88*(A8), 6289-6300. https://doi.org/10.1029/JA088iA08p06289

Ren, Z., Wan, W., Liu, L., Chen, Y., & Le, H. (2011). Equinoctial asymmetry of ionospheric vertical plasma drifts and its effect on F-region plasma density. *Journal of Geophysical Research: Space Physics*, *116*(A2). https://doi.org/10.1029/2010JA016081

Rishbeth, H., & Edwards, R. (1989). The isobaric F2-layer. *Journal of Atmospheric and Terrestrial Physics*, *51*(4), 321-338. https://doi.org/10.1016/0021-9169(89)90083-4

Rishbeth, H., Müller-Wodarg, I., Zou, L., Fuller-Rowell, T., Millward, G., Moffett, R., … Aylward, A. (2000). *Annual and semiannual variations in the ionospheric F2-layer: II. Physical discussion* (pp. 945-956). Presented at the Annales Geophysicae, Springer. https://doi.org/10.1007/s00585-000-0945-6

Roble, R. (1983). Dynamics of the Earth's thermosphere. *Reviews of Geophysics*, *21*(2), 217-233. https://doi.org/10.1029/RG021i002p00217

Roble, R., Dickinson, R. E., & Ridley, E. (1977). Seasonal and solar cycle variations of the zonal mean circulation in the thermosphere. *Journal of Geophysical Research*, *82*(35), 5493-5504. https://doi.org/10.1029/JA082i035p05493

Sahai, Y., Becker-Guedes, F., Fagundes, P., Lima, W., Otsuka, Y., Huang, C.-S., … Bolzan, M. (2007). Response of nighttime equatorial and low latitude F-region to the geomagnetic storm of August 18, 2003, in the Brazilian sector. *Advances in Space Research*, *39*(8), 1325-1334. https://doi.org/10.1016/j.asr.2007.02.064

Simon, P. A., & Legrand, J.-P. (1989). Solar cycle and geomagnetic activity: A review for geophysicists. Part II. The solar sources of geomagnetic activity and their links with sunspot cycle activity, *7*(6), 579-594.

Thrane, E. V. (1964). *Electron Density Distribution in Ionosphere and Exosphere: Proceedings*. North-Holland Publishing Company.

Titheridge, J. (1973). The electron content of the southern mid-latitude ionosphere, 1965–1971. *Journal of Atmospheric and Terrestrial Physics*, *35*(5), 981-1001. https://doi.org/10.1016/0021-9169(73)90077-9

Torr, M. R., & Torr, D. (1973). The seasonal behavior of the F2-layer of the ionosphere. *Journal of Atmospheric and Terrestrial Physics*, *35*(12), 2237-2251. https://doi.org/10.1016/0021-9169(73)90140-2

Torr, M., Torr, D., & Hinteregger, H. (1980). Solar flux variability in the Schumann-Runge continuum as a function of solar cycle 21. *Journal of Geophysical Research: Space Physics*, *85*(A11), 6063-6068. https://doi.org/10.1029/JA085iA11p06063

Venkatesh, K., Fagundes, P. R., Prasad, D. V., Denardini, C. M., De Abreu, A., De Jesus, R., & Gende, M. (2015). Day-to-day variability of equatorial electrojet and its role on the day-to-day characteristics of the equatorial ionization anomaly over the Indian and Brazilian sectors. *Journal of Geophysical Research: Space Physics*, *120*(10), 9117-9131. https://doi.org/10.1002/2015JA021307

Venkatesh, K., Fagundes, P., de Jesus, R., De Abreu, A., Pillat, V., & Sumod, S. (2014). Assessment of IRI-2012 profile parameters by comparison with the ones inferred using NeQuick2, ionosonde and FORMOSAT-1 data during the high solar activity over Brazilian equatorial and low latitude sector. *Journal of Atmospheric and Solar-Terrestrial Physics*, *121*, 10-23. https://doi.org/10.1016/j.jastp.2014.09.014

Venkatesh, K., Fagundes, P., Seemala, G. K., de Jesus, R., de Abreu, A., & Pillat, V. (2014). On the performance of the IRI−2012 and NeQuick2 models during the increasing phase of the unusual 24th solar cycle in the Brazilian equatorial and low−latitude sectors. *Journal of Geophysical Research: Space Physics*, *119*(6), 5087-5105. https://doi.org/10.1002/2014JA019960

Walker, G., Ma, J., & Golton, E. (1994). *The equatorial ionospheric anomaly in electron content from solar minimum to solar maximum for South East Asia* (pp. 195-209). Presented at the Annales Geophysicae, Springer. https://doi.org/10.1007/s00585-994-0195-0

Yonezawa, T. (1971). The solar-activity and latitudinal characteristics of the seasonal, non-seasonal and semi-annual variations in the peak electron densities of the F2-layer at noon and at midnight in middle and low latitudes. *Journal of Atmospheric and Terrestrial Physics*, *33*(6), 889-907. https://doi.org/10.1016/0021-9169(71)90089-4

Zakharenkova, I., Cherniak, I. V., Krankowski, A., & Shagimuratov, I. (2013). Analysis of electron content variations over Japan during solar minimum: Observations and modeling. *Advances in Space Research*, *52*(10), 1827-1836. https://doi.org/10.1016/j.asr.2012.09.043

Zhao, B., Wan, W., Liu, L., Mao, T., Ren, Z., Wang, M., & Christensen, A. (2007). *Features of annual and semiannual variations derived from the global ionospheric maps of total electron content* (pp. 2513-2527). Presented at the Annales Geophysicae, Copernicus GmbH. https://doi.org/10.5194/angeo-25-2513-2007

Zou, L., Rishbeth, H., Müller-Wodarg, I., Aylward, A., Millward, G., Fuller-Rowell, T., … Moffett, R. (2000). *Annual and semiannual variations in the ionospheric F2-layer. I. Modelling* (pp. 927-944). Presented at the Annales Geophysicae, Copernicus GmbH. https://doi.org/10.1007/s00585-000-0927-8

Zoundi, C., Ouattara, F. M., Fleury, R., Amory-Mazaudier, C., & Lassudrie-Duchesne, P. (2012). Seasonal TEC variability in West Africa equatorial anomaly region. *European Journal of Scientific Research*, *77*(3), 309-319.

Copyrights